Supporting information

High-Performance Polydiacetylene Organic Cathode for Zinc-Ion Batteries

Anita Samage [a], *Elinor Slavsky* [a], *Raz Jelinek** [a,b]

[a]Department of Chemistry, Ben Gurion University of the Negev, Beer Sheva 8410501, Israel

[b]Ilse Katz Institute for Nanotechnology, Ben Gurion University of the Negev, Beer Sheva 8410501, Israel

E-mail: razj@bgu.ac.il

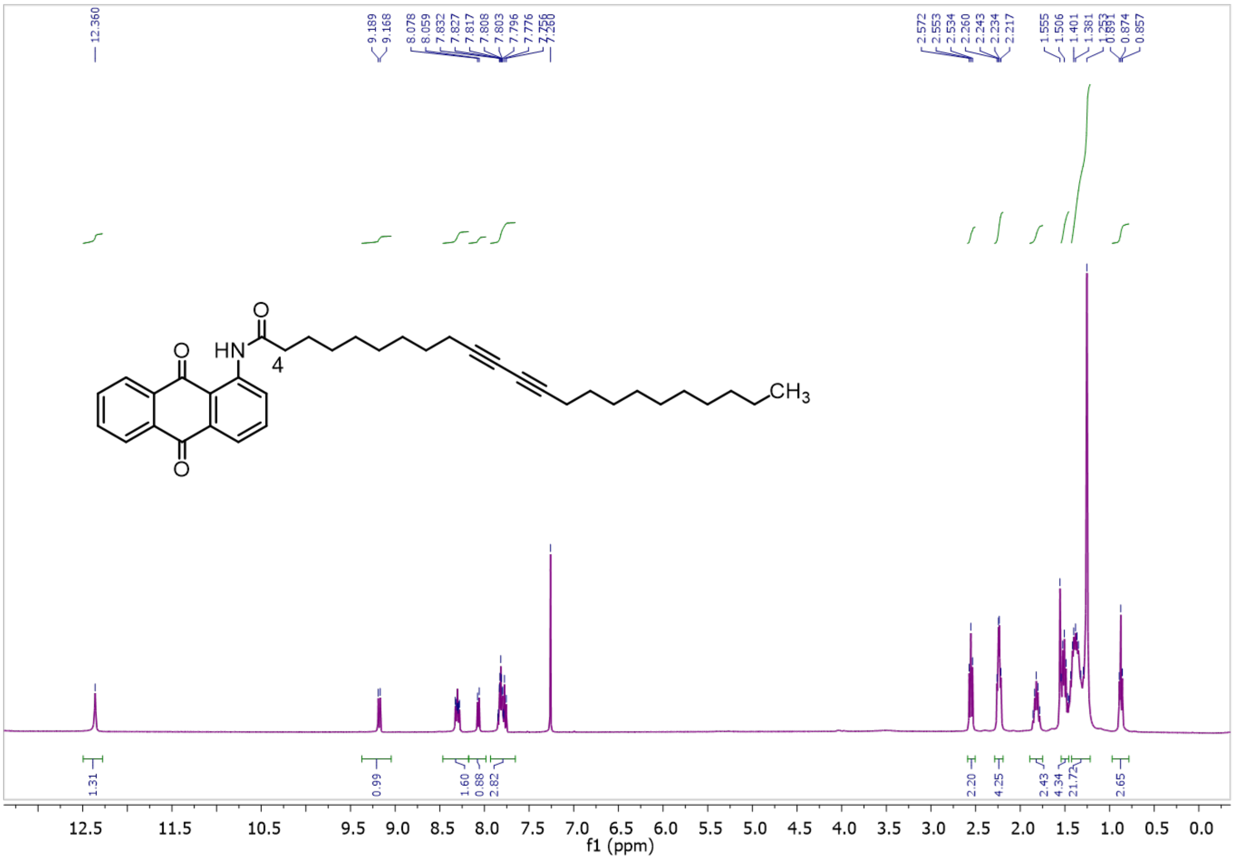

Figure S1. Proton Nuclear Magnetic Resonance (^{1}H NMR) of AQ-DA, ^{1}H NMR (400 MHz, CDCl3) δ 12.36 (s, 1H), 9.18 (dd, J = 8.6, 1.2 Hz, 1H), 8.08 (m, 2H), 8.05 (dd, J = 7.6, 1.2 Hz, 1H), 7.83 -7.75 (m, 2H), 7.77 (dd, J = 11.6, 4.6 Hz, 1H), 2.57 -2.53 (m, 2H), 2.26 – 2.21 (m, 4H), 1.81 (dd, J = 14.9, 7.4 Hz, 2H), 1.50 (dd, J = 14.8, 7.2 Hz, 4H), 1.40 -1.25 (m, 22H), 0.87 (t, J = 6.9 Hz, 3H).

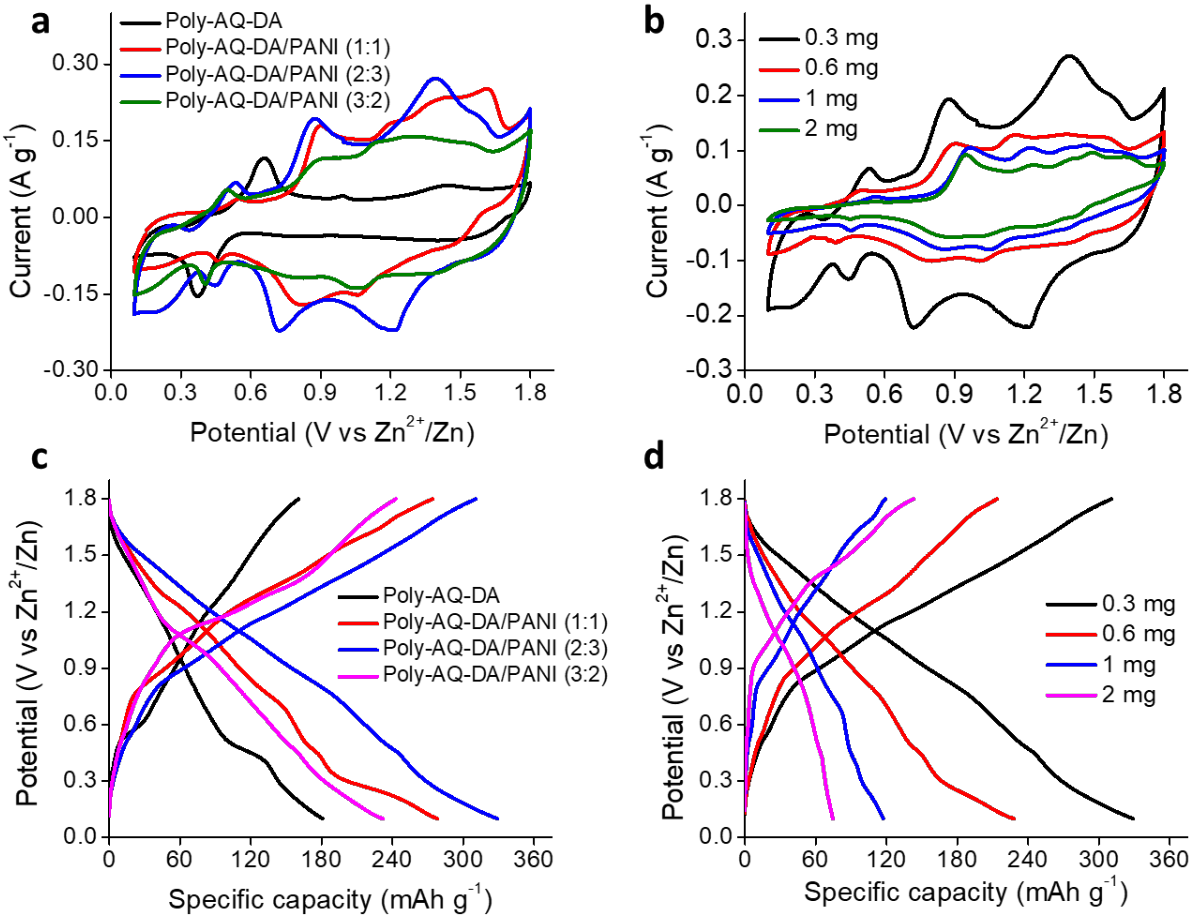

Figure S2. a) Cyclic voltammetry of (a) Different compositions of AQ-DA and PANI at 0.2 mV s^{-1}. (b) different loading of active masses (0.3 mg to 2 mg) at 0.2 mV s^{-1}. Galvanostatic charge discharge curves of c) Various compositions of AQ-DA and PANI at 0.1 A g^{-1}. (d) Different loading of active masses (0.3 mg to 2 mg) at 0.1 A g^{-1}.

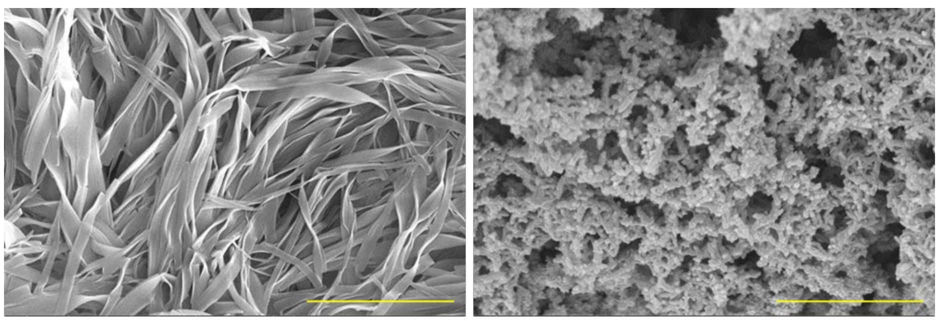

Figure S3. SEM images of poly-AQ-DA (left) and PANI (right), the scale bar corresponds to 5 μm

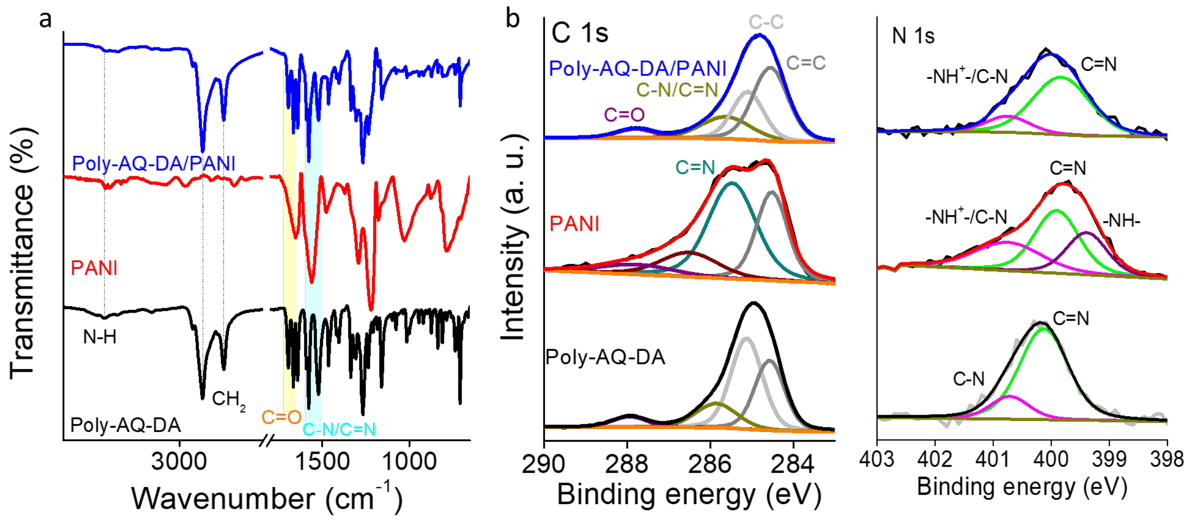

Figure S4. (a) FTIR spectra of poly-AQ-DA (black), PANI (red), and Poly-AQ-DA/PANI (blue), (b) High-resolution XPS spectra of poly-AQ-DA (bottom), PANI (middle), poly-AQ-DA/PANI (top) deposited on graphite sheet. The FTIR spectra of poly-AQ-DA/PANI and its individual components in Figure S4a corroborate the SEM data, indicating that incorporation of PANI did not interfere with the molecular structure and organization of the PDA moieties in the mixture. Specifically, no significant changes in the spectral features of poly-AQ-DA were observed in the composite poly-AQ-DA/PANI (Figure S4a, blue spectrum) as compared to only poly-AQ-DA (Figure S4a, black spectrum). Similar interpretation is apparent in the XPS results (S4b) in the poly-AQ-DA/PANI composite, the C 1s spectrum closely resembles that of poly-AQ-DA, indicating that the carbon environment is dominated by the poly-AQ-DA framework with overlapping contributions from PANI. In the N 1s spectrum, the peak of poly-AQ-DA at ~400.2 eV appears at ~399.8 eV in the composite, which coincides with the amine/imine nitrogen species of PANI, confirming the coexistence of PANI and poly-AQ-DA within the composite (figure S4b, N1s).

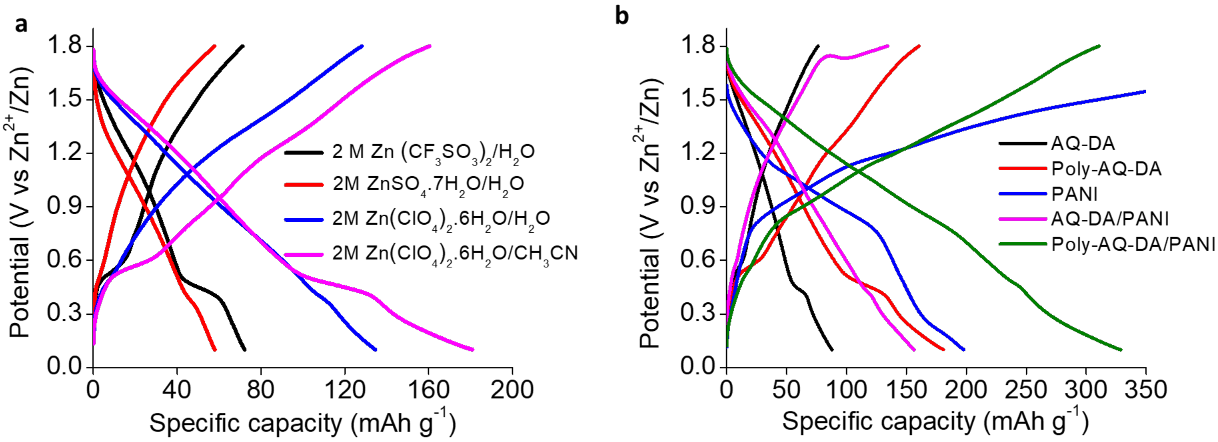

Figure S5. Galvanostatic charge-discharge curves of (a) poly-AQ-DA in different electrolytes at 0.1 A g^{-1}, (b) Individual and composite cathodes in selected 2 M $Zn(ClO_4)_2.6H_2O$ electrolyte at 0.1 A g^{-1}

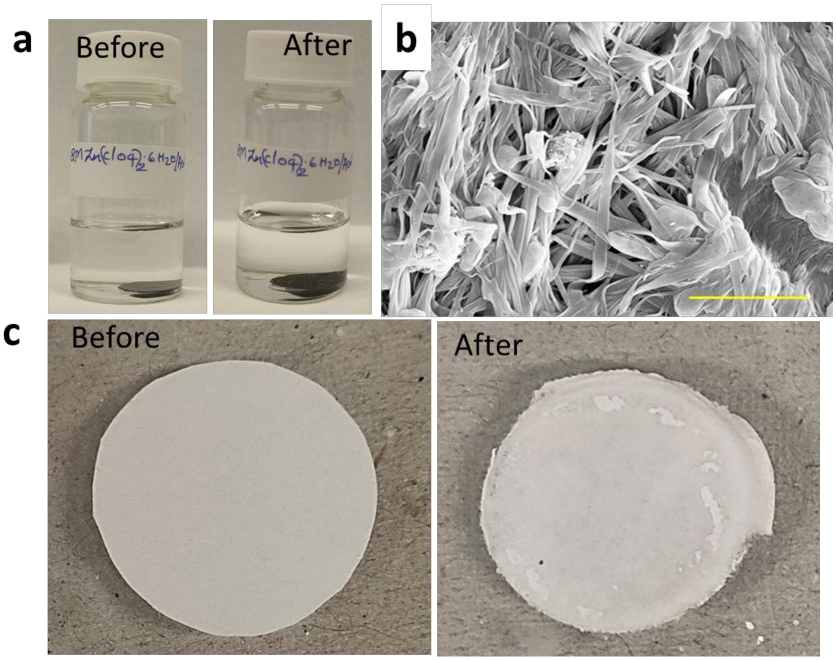

Figure S6. (a) Digital photographs of the fresh electrolyte and the electrode after soaking for 350 h, (b) SEM image of poly-AQ-DA/PANI after 350 h self-discharge profile, (c) digital photographs of the separator before and after self-discharge

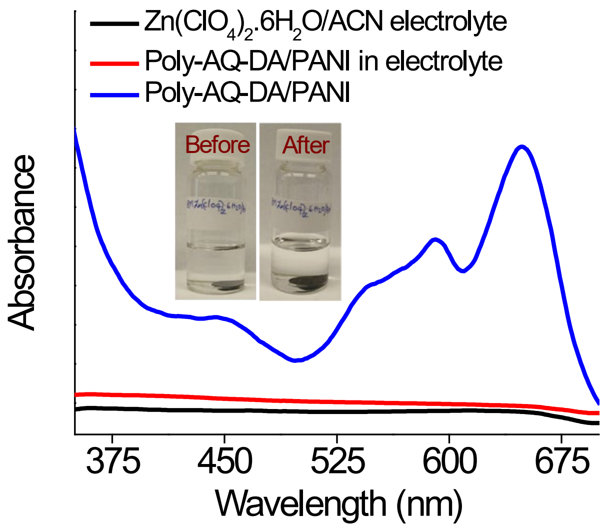

Figure S7. Ultraviolet-visible (UV-vis) spectroscopy of fresh electrolyte (black), after soaking the poly-AQ-DA/PANI electrode (red), and poly-AQ-DA/PANI electrode (blue)

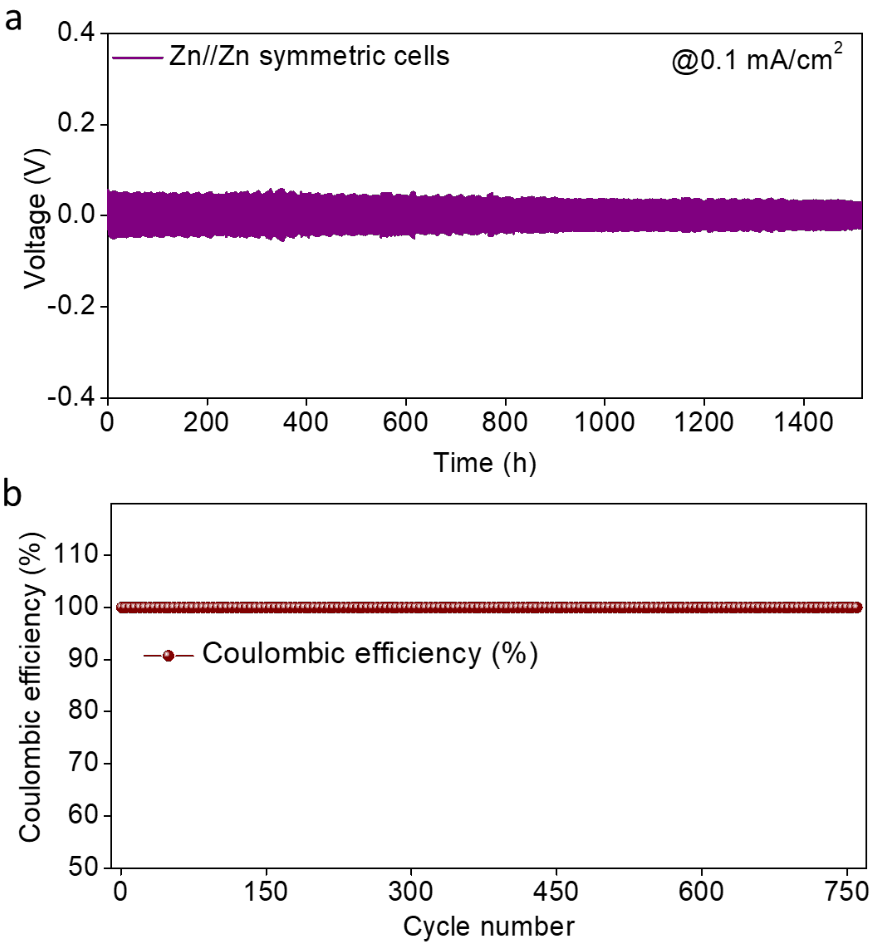

Figure S8: Stability of zinc anode in 2M $Zn(ClO_4)_2$. $6H_2O$ in acetonitrile (a) Charge-discharge cycling of Zn//Zn symmetric cell at 0.1 mA cm^{-2}. (b) Coulombic efficiency of Zn//Zn symmetric cell

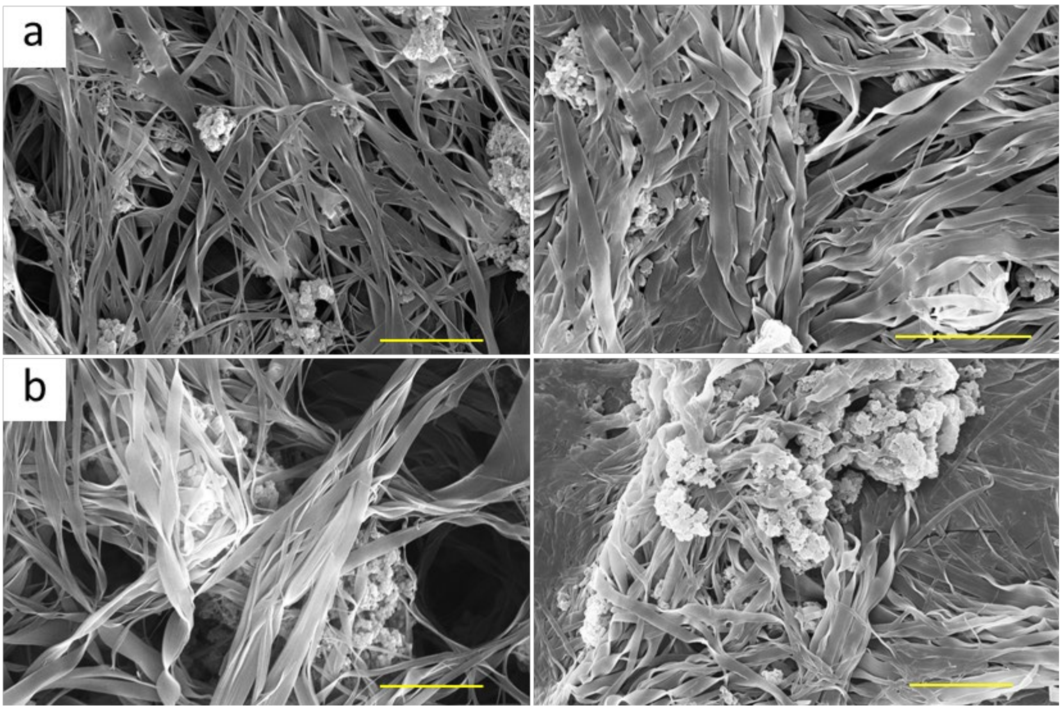

Figure S9. SEM image of poly-AQ-DA / PANI. The scale bar corresponds to 5 µm. (a) SEM images before stability (left) and after 19000 cycles at 1 A g^{-1} (right). (b) SEM images before (left) and after 1000 cycles at 0.1 A g^{-1} (right)

Table S1. Comparison of specific capacities of individual components of cathodes

Sl. No.	**Material**	**Specific capacity (mAh g^{-1}) at 0.1 A g^{-1}**
1	AQ-DA	88
2	Poly-AQ-DA	180
3	PANI	197
4	AQ-DA/PANI (2:3)	134

5	Poly-AQ-DA/APNI (2:3)	330